Attitude Control System Design of a Seated Stair Lift on a Single Rail by Using Two-Degrees-of-Freedom Control

Mitsuo Hirata, Akio Setoyama, Shuichi Adachi, and Hiroshi Sakaniwa

Abstract Stair lifts, mobile chair-like transportation devices designed to be attached to the walls of existing stairways, allow improved access between floors in private homes and have improved the quality of life for many people with mobility problems. Recently, a stair lift that utilizes a single rail has been developed as part of efforts to reduce production costs as well as construction time. However, when operating this device, it is necessary to control the horizontal seating surface in real-time by use of an actuator. In this paper, a two-degrees-of-freedom control system operated by a sliding mode controller is used to improve the overall control performance of the new stair lift. The effectiveness of the controller is verified by experiments.

1 Introduction

As a means to improve their general welfare and comfort, seated stair lifts are often used by disabled or elderly persons when ascending or descending stairs at home. Modern stair lifts can easily be installed in most existing houses and their costs are relatively low when compared with residential elevators. Normally, such stair lifts have two rails in order to mechanically ensure the seat remains horizontal when transporting a passenger. However, two-rail systems are difficult to install in a way that keeps both rails sufficiently parallel, particularly if the structure of the exist-

Mitsuo Hirata
Utsunomiya University, 7-1-2 Yoto, Utsunomiya, Tochigi 321-8585, Japan

Akio Setoyama
Utsunomiya University, 7-1-2 Yoto, Utsunomiya, Tochigi 321-8585, Japan

Shuichi Adachi
Keio University, 3-14-1 Hiyoshi, Kohoku-ku, Yokohama, Kanagawa 223-8522, Japan

Hiroshi Sakaniwa
Syntex Co., Ltd., 1114 Kitsuregawa, Sakura, Tochigi 329-1412, Japan

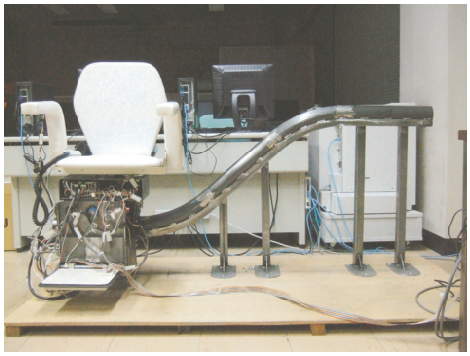

Fig. 1 Seated stair lift on a single rail

ing stairway is complex. Thus, we have developed a stair lift that utilizes a single rail, as shown in Fig.1. Use of this stair lift can reduce production costs as well as construction time.

One difficult aspect in the design of the single-rail stair lift was the need to control the horizontal positioning of the seat in real-time by use of an actuator [1, 4]. In order to ensure the passenger's safety and comfort, the level of the seat needs to be kept to within plus or minus 0.5 degrees of horizontal. However, this is sometimes difficult to control, especially in situations where the rail angle changes drastically. We therefore determined that the chair's control system needed to be designed with good transient response. In addition, it was also important for the system to be sufficiently robust with respect to uncertainties associated with the seat level actuator exhibiting dead-zone nonlinearity at the plant input, and because the weight of the passenger can be expected to vary.

In this paper, a two-degrees-of-freedom (TDOF) control scheme is used to improve the transient response of the seating face angle. In this TDOF control sys-

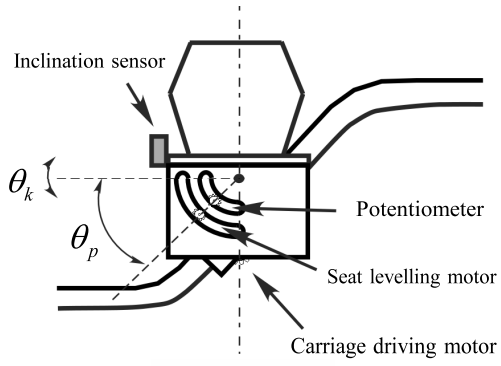

Fig. 2 Schematic diagram of plant

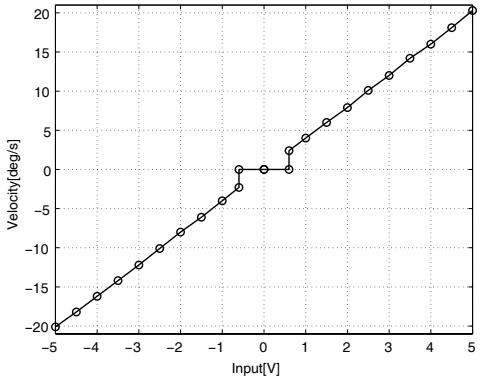

Fig. 3 Dead-zone nonlinearity of DC motor

tem, the sliding mode control (SMC) method [2] is used as the feedback controller because of its effectiveness in completely suppressing matched uncertainties such as input nonlinearity and/or input disturbances. The effectiveness of the proposed method is verified by experiments.

2 Seated stair lift modeling

2.1 Seated stair lift configuration

As shown in Fig.2, the stair lift consists of a carriage and seat designed to move along a single rail that is mounted on the wall of an existing stairway. The relative angle between the carriage and the seat can be adjusted by use of a brushless, velocity control type DC motor that is capable of being operated with lead acid batteries.

The control input is a reference to the motor velocity, and the DC motor has a dead-zone nonlinearity at the plant input, as shown in Fig.3. The motor cannot be moved by a reference input lower than ± 0.58 V because it was originally designed for constant velocity use and is not well optimized for performance at lower velocities. While it is true that there are numerous motors that have good lower velocity properties, their usage was decided against because of cost.

The output, which is a relative angle θ_p between the carriage and the seat, is measured by a potentiometer. The inclination of the seat θ_k is measured by an inclination sensor. The position of the carriage from the initial position on the rail is measured by a rotary encoder, and the initial position of the carriage is detected by a limit switch.

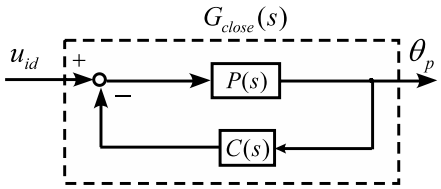

Fig. 4 Closed-loop system for system identification

2.2 System identification

A system identification method that can construct a model of the plant from input and output data is used [3]. The plant input is the reference to the motor velocity, while its output is the relative angle θ_p. Since the system has an unstable pole at the origin that corresponds to the integrator between velocity and position, the plant is stabilized by a unity feedback controller $C(s) = 1$ as shown in Fig.4. The time response of the relative angle θ_p is obtained by adding the external identification input u_{id}. The second-order ARMAX model $G_{close}(s)$ is identified by the obtained input and output data, and the transfer function of the plant $P(s)$ is given by $P(s) = G_{close}(s)/(1 - G_{close}(s)C(s))$. Given that the plant should have a pole at the origin, the pole of the identified plant near the origin was substituted by an integrator. Finally,

$$P(s) = \frac{0.167(s+12.1)}{s(s+4.18)} \tag{1}$$

is obtained. This can be transformed to the controllability canonical form

$$\begin{cases} \dot{x}_p = \begin{bmatrix} 0 & 1 \\ 0 & a_{22} \end{bmatrix} x_p + \begin{bmatrix} 0 \\ 1 \end{bmatrix} u, \quad x_p = \begin{bmatrix} x_1 \\ x_2 \end{bmatrix} \\ y = \begin{bmatrix} c_1 & c_2 \end{bmatrix} x_p \end{cases} \tag{2}$$

where $a_{22} = -4.18$, $c_1 = 28.8$, and $c_2 = 1.70$.

2.3 Measurement of rail angle

In the TDOF control system, a rail angle is required as the reference to the relative angle θ_p. The rail angle is measured by the inclination sensor fixed to the seat, while the relative angle θ_p is kept at 0 deg and the carriage is moved at a very slow speed so as not to induce unexpected dynamics into the inclination sensor. The measurement noise is then removed by a low-pass filter, and the amount of data is reduced to ease

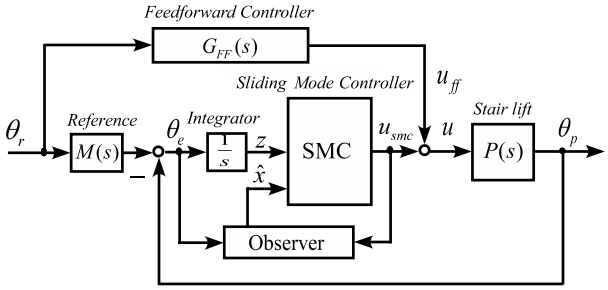

Fig. 5 Two-degrees-of-freedom control system

demands on the memory of the on-board computer. A mapping table that represents the relation between the carriage position and the rail angle is then created.

3 Control system design

3.1 Model matching two-degrees-of-freedom control system

In this paper, the model matching two-degrees-of-freedom control system as shown in Fig.5 is used to improve the transient response. In Fig.5, G_{FF} is a feedforward controller and M is a reference model. The transfer function from θ_r to θ_p coincides with M by choosing $G_{FF} = M/P$. The reference model M is selected to satisfy $|M(j\omega)| \simeq 1$ over the control bandwidth.

In this paper, the transfer function of M is given by

$$M(s) = \frac{\omega_n^2}{s^2 + 2\zeta\omega_n s + \omega_n^2}$$

where the natural frequency ω_n and the damping ratio ζ are design parameters.

If a disturbance or uncertainty occurs, the feedback controller works to minimize the tracking error θ_e. In this research, the SMC is used. Since the SMC requires information on all the plant states, those estimates are provided by a state observer.

3.2 Sliding mode controller

3.2.1 Matched disturbance

In the plant modeling, the plant is assumed to be linear. However, the DC motor has a dead-zone nonlinearity at the plant input as shown in Fig.3. The nonlinearity at

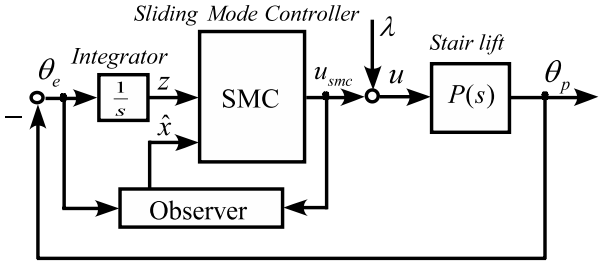

Fig. 6 SMC system with matched disturbance

the plant input can be regarded as an equivalent disturbance at the plant input. This type of equivalent disturbance acting on the plant input is referred to as *matched disturbance* and the SMC method is capable of completely eliminating the effects of a matched disturbance.

3.2.2 Design of hyperplane

Since the SMC is used in the TDOF control framework, it only works when $\theta_e \neq 0$. Therefore, the block diagram of Fig.6 is considered by assuming $\theta_r = 0$ in Fig.5. In Fig.6, λ represents the matched disturbance acting on the plant input.

The state variable of the integrator is introduced

$$z = -\int_0^t y\, dt. \tag{3}$$

Thus from Eq.(2) and Eq.(3), the state space form of the augmented system of Fig.6 is given by

$$\begin{aligned} \dot{x} &= \left[\begin{array}{cc:c} 0 & -c_1 & -c_2 \\ 0 & 0 & 1 \\ \hdashline 0 & 0 & a_{22} \end{array}\right] x + \left[\begin{array}{c} 0 \\ 0 \\ \hdashline 1 \end{array}\right] (u_{smc} + \lambda) \\ &= \left[\begin{array}{cc} A_{11} & A_{12} \\ 0 & a_{22} \end{array}\right] x + \left[\begin{array}{c} 0 \\ 1 \end{array}\right] (u_{smc} + \lambda) \end{aligned} \tag{4}$$

where $x = [z,\, x_p^T]^T = [z,\, x_1,\, x_2]^T = [{x_{eq}}^T,\, x_2]^T$. The output equation is given by

$$y = \theta_p = \left[\begin{array}{cc:c} 0 & -c_1 & -c_2 \end{array}\right] x = \left[\begin{array}{cc} C_1 & c_2 \end{array}\right] x.$$

The switching function of the SMC is given by $\sigma = \left[\begin{array}{cc:c} s_1 & s_2 & s_3 \end{array}\right] x = \left[\begin{array}{cc} S_1 & s_3 \end{array}\right] x$.

When the state variables of the system are constrained on the sliding surface, the matched disturbance is completely removed and the state x_2 of the system Eq.(4) can be removed to reduce the order of the system, which can be obtained as follows:

$$\dot{x}_{eq}(t) = (A_{11} - {s_3}^{-1} A_{12} S_1) x_{eq}(t) = \tilde{A} x_{eq}(t). \tag{5}$$

All the states of the reduced-order system Eq.(5) go to zero if the parameters s_1, s_2, and s_3 are selected so that $\tilde{A}$ is Hurwitz.

3.2.3 Design of sliding mode controller

In this research, an eventual SMC method is used. The control input u_{smc} of the SMC is given by

$$u_{smc} = u_l + u_{nl}$$

where u_l and u_{nl} are linear and nonlinear inputs, respectively. The linear input u_l is given by

$$u_l = -(SB)^{-1} SAx$$

where A, B, and S are defined by

$$A = \begin{bmatrix} A_{11} & A_{12} \\ 0 & a_{22} \end{bmatrix}, \; B = \begin{bmatrix} 0 \\ 1 \end{bmatrix}, \; S = \begin{bmatrix} S_1 & s_2 \end{bmatrix}.$$

Conversely, the nonlinear input is given by

$$u_{nl} = -K(SB)^{-1} \frac{\sigma}{||\sigma||}$$

where K is a switching gain.

The switching gain is determined by using a Lyapunov function. A candidate for the Lyapunov function is given by $V = (1/2)\sigma^2$. The time derivative of V along the closed-loop trajectories is given by

$$\dot{V} = -K \frac{\sigma^2}{||\sigma||} + SB\lambda \; \sigma \; < \; 0. \tag{6}$$

From $\lambda \; \sigma \leq |\lambda| \; |\sigma|$, the sufficient condition of Eq.(6) becomes

$$K \; > \; SB|\lambda|.$$

Assuming that the matched disturbance has an upper bound ρ that satisfies $|\lambda| \; \leq \; \rho$, the lower bound of K is given by

$$K \; > \; SB\rho. \tag{7}$$

For practical reasons, a smooth function is also introduced in order to prevent unexpected chattering.

Table 1 Design parameters

Parameters	Values
Eigenvalues of $\tilde{A}$	$[-9, -10]$
Hyper plane S	$[-4.4, 11.6, 1.00]$
Gain K	2.0
Observer poles	$[-20, -25]$
Parameters of reference model	$\zeta = 0.66$, $\omega_n = 10$
Input limitation	$\pm$5V

4 Experiments

4.1 Design parameters

The design parameters are summarized in Table 1. The poles of the state observer are selected to ensure that the estimation error of the plant output is smaller than ± 0.5 deg in order to achieve the control requirement of ± 0.5 deg. The parameters ζ and ω_n of the reference model M are selected to ensure that carriage vibration does not occur, and that a smooth response is obtained.

The eigenvalues of $\tilde{A}$ that determines the dynamics of the sliding motion are selected after considering the balance between the linear and nonlinear inputs of the SMC. At the same time, a check is made to ensure the state variables are constrained on the sliding surface and that the linear input is not oscillating.

The switching gain K has to be determined so as to satisfy Eq.(7). However, a larger gain may result in chattering phenomena, while a smaller gain may not be sufficiently robust to counteract the input nonlinearity and/or weight change of passengers. In this research, K is adjusted in order to be sufficiently robust to accommodate a passenger whose weight is about 60 kg.

4.2 Experimental results

The controller was discretized with a sampling period of 10 ms and applied to the attitude control system of the seated stair lift. The control performance was evaluated by moving the carriage while transporting a passenger weighing about 60 kg. The time response of θ_p is shown in the upper of Fig.7. The error $\theta_e = \overline{\theta}_r - \theta_p$, where $\overline{\theta}_r$ is the output of M and θ_p is the relative angle, is shown in the middle of Fig.7. In a comparison test, the sliding mode controller was replaced by a PID controller, and the same experiment was repeated. The PID gains were tuned manually, and with some trial and error, were capable of good control performance. It follows that P gain is 1.2, I gain is 1.4 and D gain is 0.2.

From Fig.7, it was found that the sliding mode controller reduces error to within ± 0.4 deg, and good performance can be achieved compared with the PID controller.

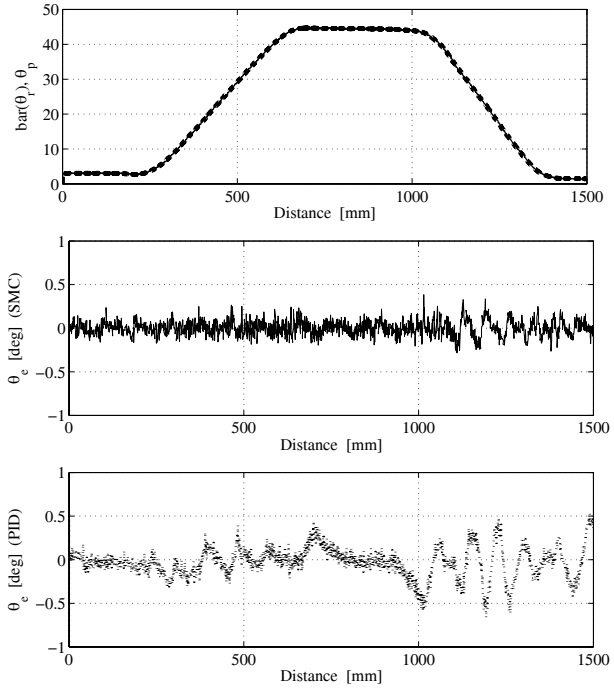

Fig. 7 Experimental results (solid line: sliding mode control, dotted line: PID control, dashed line: reference)

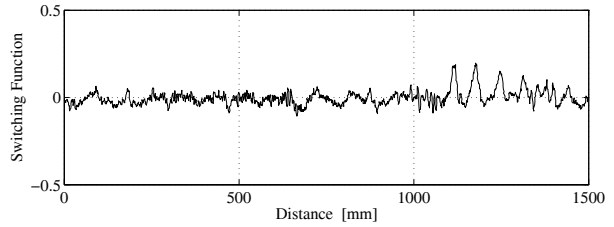

Fig. 8 Switching function

Fig.8 shows the time response of the switching function, and it can be seen that there were some differences in the response at the position of 250∼700 mm and 1100∼1500 mm, where the rail angle changes. It can be considered that the effect of gravity acting on the seat is increased at the latter portion because of the structure of the seated stair lift.

The upper and the lower figures of Fig.9 show the time response of the feedforward and feedback inputs, respectively. However, the feedforward input is dominant and the magnitude of the feedback control input was also increased in order to minimize the errors that tend to occur at the position where the rail angle changes.

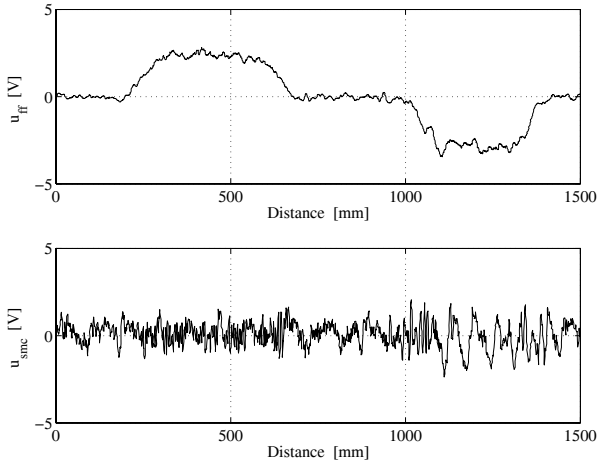

Fig. 9 Control input (upper: feedforward input, lower: feedback input)

Ride quality is also important. The sliding mode controller achieved good ride quality in comparison with the PID controller because it maintained the seat surface in a horizontal position more precisely and there was no persistent oscillation due to chattering.

5 Summary

In this research, a TDOF controller equipped with SMC has been applied to the seat attitude control of a seated stair lift. The plant model was obtained by the system identification method. The SMC controller was designed and incorporated to suppress the dead-zone nonlinearity of the DC motor. The effectiveness of the proposed control system was verified by experiments. As for future work, the control algorithm as well as the mechanism of the seated stair lift itself will be refined to improve control performance.

References

1. Ashikawa, M., Hirata, M., Adachi, S., Sakaniwa, H.: Attitude Control Systems Design of Seated Stairlift on the Single Rail by Robust Control Theory, Proc. of the 12th term JSME Kanto Branch General Meeting, pp.305–306 (2006) (in Japanese)
2. Edwards, M., Spurgeon, S.K.: Sliding Mode Control — Theory and Applications, CRC Press (1998)
3. Ljung, L.: System Identification – Theory for the User (2nd ed.), Prentice Hall (1999)
4. Setoyama, A., Hirata, M., Adachi, S., Sakaniwa, H.: Attitude Control Systems Design of Seated Stairlift on the Single Rail by Using Two-Degrees-of-Freedom Control, Proc. of the 13th term JSME Kanto Branch General Meeting, pp.19–20 (2007) (in Japanese)